Journal of Chromatography, 288 (1984) 1–14
Elsevier Science Publishers B.V., Amsterdam — Printed in The Netherlands

CHROM. 16,489

DYNAMIC PHENOMENA DURING ENANTIOMER RESOLUTION BY COMPLEXATION GAS CHROMATOGRAPHY

A KINETIC STUDY OF ENANTIOMERIZATION

WALDEMAR BÜRKLE, HEINRICH KARFUNKEL and VOLKER SCHURIG*
Fakultät für Chemie und Pharmazie, Universität Tübingen, Auf der Morgenstelle, D 7400 Tübingen (F.R.G.)
(Received November 26th, 1983)

SUMMARY

A peak form analysis is presented which describes the elution profiles of interconverting enantiomers during their resolution on a chiral stationary phase in a gas chromatographic column. An equation has been derived which permits for the first time the quantitative assessment of peak distortions arising from enantiomerization occurring in the stationary phase. The simulated peak shapes represent a means of diagnosing configurational inversion during gas chromatographic enantiomer resolution, which is a source of error in the determination of enantiomeric compositions. For the invertomers of 1-chloro-2,2-dimethylaziridine the activation barrier in the presence of the resolving stationary phase nickel(II) bis[3-(trifluoroacetyl)-1*R*-camphorate] in squalane has been determined to be $\Delta G^{\neq} = 104.9 \pm 0.6$ kJ/mol.

INTRODUCTION

It is well established that, when partitioned between a mobile and stationary phase, the latter being chiral (and enantiomerically pure), optical isomers (enantiomers) may show considerable differences and can therefore be resolved, *e.g.*, by gas[1,2] or liquid chromatography[3–5]. Hitherto, only those enantiomers have been separated which retain their stereochemical integrity during the entire resolution process. Here we describe, both experimentally and theoretically, elution patterns which arise when configurationally labile enantiomers are chromatographed on a chiral resolving stationary phase.

We adopt the term "enantiomerization" to characterize a process in which the individual antipodes of a racemic or enriched mixture of enantiomers undergo inversion of their respective configurations during chromatographic resolution. It had previously been inferred[6] that the dynamic behaviour of interconverting enantiomers will result in intrinsic distortions of the elution curves amenable to the acquisition of kinetic data by peak form analysis. It is noted in this context that the equilibrium of inversion of configuration of enantiomers

$$p \rightleftarrows q$$

0021-9673/84/$03.00

is governed by entropic changes, only, and that it represents a simple case of a reversible unimolecular reaction. In regard to experimental quantitation, the present system is especially appealing as (achiral) chromatographic detectors respond identically to optical isomers. Enantiomerization, as a first-order reaction, is therefore ideally suited for kinetic study by "reaction gas chromatography"[7,8].

The recent introduction of "complexation gas chromatography"[2] utilizing chiral transition metal co-ordination compounds as enantiospecific stationary phases for the resolution of racemic Lewis-base substrates enabled us for the first time to investigate the chromatographic behaviour of the configurationally labile aziridine invertomers 1 (with chirality due to pyramidally coordinated asymmetric nitrogen).

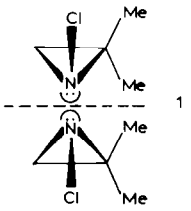

1

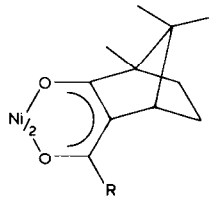

2 R = CF_3
3 R = $CF_2CF_2CF_3$

In the present investigation the elution patterns of the invertomers of 1 undergoing configurational change during chromatographic resolution are computer simulated. Simulated and observed chromatograms are compared using an approximate method based on peak height ratios. The best fit between the simulated and experimental interconversion profiles provides the rate constant and the free enthalpy of activation of inversion for 1 proceeding in the stationary phase.

EXPERIMENTAL

Instrumentation

A Carlo Erba Fractovap 2101 instrument equipped with a flame ionization detector and suitable for wall-coated open-tubular column operation was used. High purity nitrogen, free from water and oxygen, was used as carrier gas. The splitting ratio was 1:50. The injector temperature was *ca.* 70°C above the column temperature. The solutes were injected together with methane (to determine t_M) as air-diluted vapours drawn from silicon-sealed "head-space" vials (Perkin-Elmer). The sensitivity of the instrument was set as high as possible. A 100 m × 0.5 mm nickel open-tubular column (200 seamless, 99.53% Ni, 0.24% Mn) obtained from Handy and Harmon Tube Co. (Norristown, PA, U.S.A.) was used. Prior to coating the column was washed repeatedly with methylene chloride and acetone.

Coating of the column[9]

The column was coated at room temperature by the dynamic plug method. In a typical experiment the required amount of metal chelate, 2 or 3, and 250 mg squalane (purified by filtration over active alumina) were dissolved in 3.5 ml of high purity chloroform with gentle warming when necessary. The solution was filtered through glass wool, transferred into a home-made coating device made from PTFE and passed through the column at 0.6 bar N_2. The nitrogen pressure was maintained for

10 h after the coating liquid had emerged from the column. The column was connected to the injector and conditioned for 12 h between 25 and 100°C. It has been found advantageous to flame-heat 10 cm of the column end before connecting with the detector. Care was taken to minimize dead-volumes in the entire flow system.

Metal chelates and solutes

Nickel(II) bis[3-(trifluoroacetyl)-1*R*-camphorate], 2, was prepared according to ref. 18 and nickel(II) bis [3-(heptafluorobutyryl)-1*R*-camphorate], 3, according to ref. 9. 1-Chloro-2,2-dimethylaziridine (1) was obtained via N-chlorination of 2,2-dimethylaziridine according to ref. 9.

Computer programming

Scheme I represents the calculation of the equilibrium distribution and procedures to integrate the rate equations. The simulation procedure was written in FORTRAN and BASIC. The BASIC version was implemented on a HP-9845 desk computer and the FORTRAN version on a TR-440 computer. Further details of the computer program and the derivations of the equations may be obtained from the authors on request.

RESULTS AND DISCUSSION

Two coalescence phenomena may be distinguished upon chromatography of chiral solutes on chiral stationary phases[9]:

The two separate eluates of the resolved antipodes yield peaks at the same position if the optically active stationary phase is replaced by the racemic mixture (1:1). This (trivial) phenomenon has been referred to as "peak coalescence of the first kind"[9].

The two separate eluates of the resolved antipodes gradually yield peaks at the same position as the enantiomers are rapidly inverted in molecular configuration during elution on the optically active stationary phase ("enantiomerization"). This phenomenon has been referred to as "peak coalescence of the second kind"[9]. If enantiomerization is slow, an overlapping zone ("plateau") is created between the resolved peaks. Whereas the two terminal peaks essentially arise from molecules which have retained their configuration as p or q during the entire resolution process, the interfering "plateau" originates from molecules which elute from the column as p and q, inversion of configuration occurring at least once at any part of the column.

The two coalescence phenomena are illustrated in resolution experiments on 1-chloro-2,2-dimethylaziridine (1) on nickel(II) bis[3-(trifluoroacetyl)-1*R*-camphorate], 2, in squalane solution (*cf.*, Fig. 1). Of prime importance to the present investigation is the observation that the occurrence of peak coalescence of the second kind depends on the choice of the metal chelate employed at a given temperature. Thus, coalescence was observed for 1 on 2, but not on 3 at 60°C. This result implies that the observed "dynamic" elution pattern is caused by rate-enhancing mechanisms which occur in the stationary phase only, *i.e.*, in the presence of a particular metal chelate, but not in the mobile phase, *i.e.*, under inert gas phase conditions. Indeed, Lefevre *et al.*[10] recognized that an auxiliary metal-containing probe may participate in the kinetics of enantiomerization in NMR experiments employing chiral lantha-

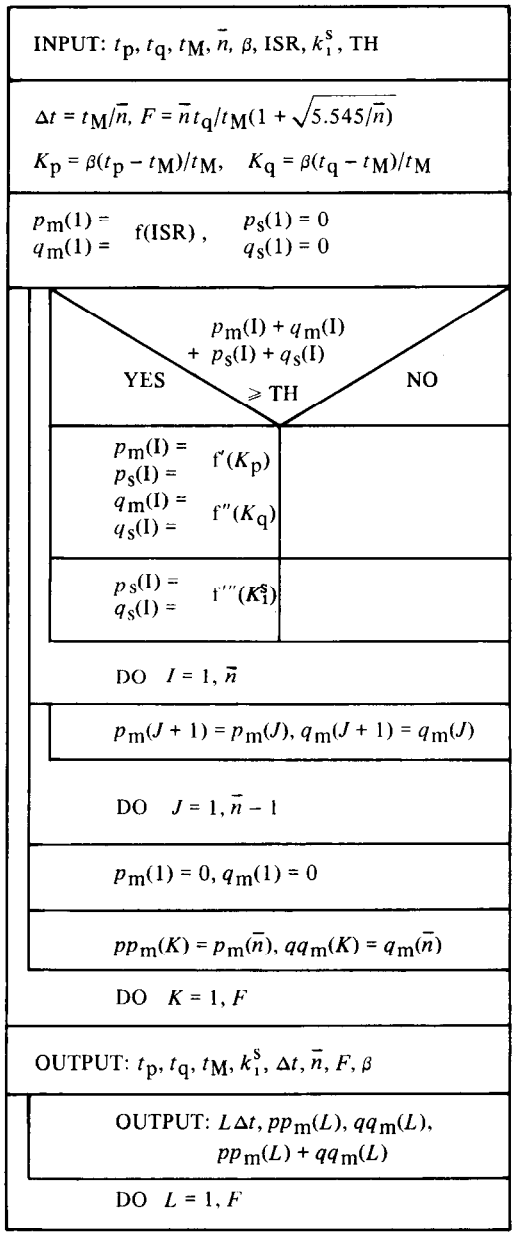

entering variables

calculating basis parameters

injection (assigning primary values to the first section)

asking for the content of section I

calculating the distribution of section I

calculating the enantiomerization in the stationary phase of section I

loop

shifting of the mobile phase to the adjacent section
loop

inert injection after shifting

storage of the eluted solutes p and q at the time $K\Delta t$
loop

output of basis parameters

plotting of the digitalized elution profile of the solutes p and q, and $p + q$ in steps Δt
loop

Scheme I.

nide shift reagents. At the present time the origin of the chromatographic rate-enhancing mechanism of inversion of 1 is unknown.

In order to use gas chromatography (GC) as a convenient tool for the evaluation of kinetic parameters of enantiomerization, we performed a computer-assisted peak form analysis for "reaction gas chromatograms" featuring peak coalescence of the second kind. A relationship between the shape of the elution curves of interconverting enantiomers

$$\mathrm{p} \underset{k_{-1}}{\overset{k_1}{\rightleftharpoons}} \mathrm{q}$$

and the rate constants k_1 and k_{-1} of the reversible first-order enantiomerization was thus established. For a given racemate, kinetic data of activation are then obtained by the comparison of experimental and computed chromatograms.

Three models, describing chromatographic separation processes, may be used for the simulation of elution curves[11], *i.e.*, the material balance or continuous flow model[7,8], the random walk model[12] and the discontinuous plate model[13]. For mathematical simplicity and ease of translation into computer language, we selected the third approach which describes chromatographic separation as a discontinuous process by assuming that all processes proceed repeatedly in separate uniform sections of a multicompartmentalized column[13]. Basset and Habgood[14] and Kallen and Heilbronner[15] have already studied and computed irreversible first-order reactions

$$\mathrm{A} \overset{k_1}{\rightarrow} \mathrm{B}$$

Scheme I.

t_p, t_q	Retention times, t_R, of solutes p and q, measured from the injection time, $t_q > t_p$
t_M	Gas hold-up time (dead-volume time)
$\bar{n}$	Number of sections in which the chromatographic column is divided (mean number of theoretical plates for p and q)
β	Phase ratio
ISR	Initial solute ratio, p/q, injected
TH	Threshold; if the content of a section is below TH the corresponding elementary steps are ignored
k_1^s	First-order rate constant for enantiomerization (isomerization) in the stationary phase
t_{max}	Maximum chromatographic time, $t_q + w_h^q$
w_h^q	Peak width at half height for q
Δt	Residence time within one section, time unit: $\Delta t = t_M/\bar{n}$
F	Maximum number of time units, $F = t_{max}/\Delta t$
I, J	Indices of the column sections
K, L	Indices of the time units
$p_m(I)$, $q_m(I)$	Concentrations of the solutes p and q in the mobile phase of the column section I
$p_s(I)$, $q_s(I)$	Concentrations of the solutes p and q in the stationary phase of the column section I
$f'(K_p)$	Functions of K_p (eqns. 2 and 3)
$f''(K_p)$	Functions of K_p (eqns. 4 and 5)
$f'''(k_1^s)$	Functions of k_1^s (eqns. 10 and 11)
K_p, K_q	Concentration-independent distribution coefficients of solutes p and q
$pp_m(K)$, $qq_m(K)$	Concentrations of the solutes p and q at the end of the column at the time K multiplied by Δt

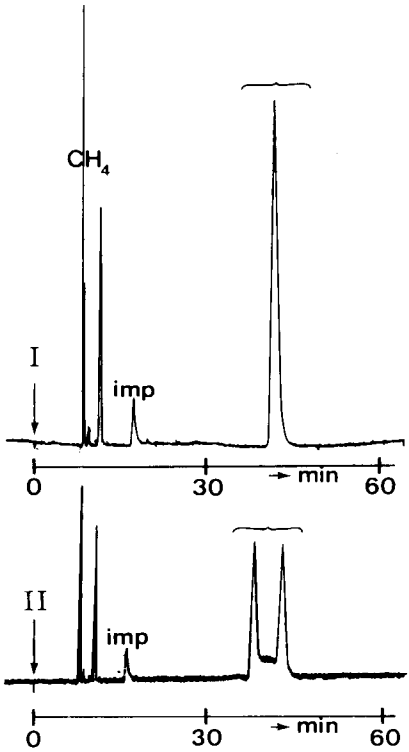

Fig. 1. Coalescence phenomena observed on complexation GC of 1-chloro-2,2-dimethylaziridine (1) on nickel(II) bis[3-(trifluoroacetyl)camphorate], 2 (0.13 *M* in squalane), at 60°C[9]. Top: peak coalescence (first kind) of 1 on racemic 2. Bottom: peak coalescence (second kind) during resolution of 1 on enantiomerically pure 1*R*-2 with the occurrence of a "plateau" between the terminal peaks. imp = impurity.

occurring in a GC reactor using the plate theory[13]. Significantly, peak broadening caused by the chromatographic process forms an integral part of the plate model.

In the present mathematical treatment of enantiomerization the dynamic processes taking place in the chromatographic reactor are separated into three steps which proceed successively in each section of the column:

establishment of the concentration-independent distribution (partitioning) equilibrium of p and q between the mobile (m) and stationary (s) phases

reversible first-order enantiomerization of the antipodes p and q in the stationary phase in the presence of the resolving sorbent during the time period, Δt

transportation (shifting) of the mobile phase to the adjacent section of the multicompartmentalized column.

Thus, the chromatographic reactor is divided into small sections the number of which is related to the number of theoretical plates, *n*. In the present treatment the height of a theoretical plate, HETP, has been chosen as the size of a section. At the start, the amounts *p* and *q* are introduced into the first section in the initial enantiomer ratio at the injection point (usually 1:1). In the first simulation step the distribution equilibria of p and q between the mobile and stationary phase are com-

puted for each section containing any quantity of the solutes, with the distribution isotherm being considered linear, *i.e.*, the partition coefficients are concentration independent. In the second step the degree of enantiomerization occurring during the residence time in the stationary phase is determined for both p and q according to a first-order rate law, and in the final step the content of the mobile phase of each section is shifted to the adjacent one. These procedures are repeated until all of the solutes have left the column.

The following arithmetic operations describe the individual steps. At the given flow-rate of the mobile phase (the pressure drop along the column is neglected, which is permissible for first-order reactions[7,8]) the residence time Δt of p and q in the mobile phase per section is:

$$\Delta t = t_2 - t_1 \tag{1}$$

Thus, Δt is the time after which the fraction of the mobile phase is shifted to the next section while the fraction of the stationary phase is retained. It is calculated as the ratio of the gas hold-up time, t_M, and the mean number of theoretical plates, $\bar{n}$, for p and q, respectively.

The distribution of p and q between the mobile (m) and stationary (s) phases is given by

$$p_m(t_2) = \frac{1}{1 + K_p}[p_m(t_1) + p_s(t_1)] \tag{2}$$

$$p_s(t_2) = \frac{K_p}{1 + K_p}[p_m(t_1) + p_s(t_1)] \tag{3}$$

$$q_m(t_2) = \frac{1}{1 + K_q}[q_m(t_1) + q_s(t_1)] \tag{4}$$

$$q_s(t_2) = \frac{K_q}{1 + K_q}[q_m(t_1) + q_s(t_1)] \tag{5}$$

where p and q represent molar concentrations of the antipodes and K_p and K_q their distribution (partition) coefficients calculated from the retention times, t_R and t_M, and the phase ratio, β.

The reversible first-order enantiomerization reaction

$$\mathrm{p} \underset{k_{-1}^s}{\overset{k_1^s}{\rightleftarrows}} \mathrm{q}$$

occurring in the stationary phase is described by

$$p_s(t_2) = \frac{k^s_{-1}}{k^s_1 + k^s_{-1}} [p_s(t_1) + q_s(t_1)] +$$

$$+ \left\{ p_s(t_1) - \frac{k^s_1}{k^s_1 + k^s_{-1}} [p_s(t_1) + q_s(t_1)] \right\} \cdot \exp [-(k^s_1 + k^s_{-1})\Delta t] \quad (6)$$

$$q_s(t_2) = \frac{k^s_1}{k^s_1 + k^s_{-1}} [p_s(t_1) + q_s(t_1)] +$$

$$+ \left\{ q_s(t_1) - \frac{k^s_1}{k^s_1 + k^s_{-1}} [p_s(t_1) + q_s(t_1)] \right\} \cdot \exp [-(k^s_1 + k^s_{-1})\Delta t] \quad (7)$$

where k^s_1 and k^s_{-1} are the rate constants for the forward and backward reactions, respectively, taking place in the stationary phase. Because enantiomerization proceeds only in the stationary phase, as implicated experimentally (*vide supra*), the following reaction scheme can be formulated:

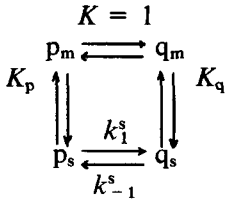

The relationship between the rate and distribution constants is determined by the "principle of microscopic reversibility" and takes the following form:

$$\frac{K_q}{K_p} = \frac{k^s_1}{k^s_{-1}} \cdot \frac{k^m_{-1}}{k^m_1} \quad (8)$$

Because $K = 1$ in the mobile phase, the ratio of the rate constants k^s_1/k^s_{-1} equals that of the distribution coefficients K_q/K_p:

$$\frac{K_q}{K_p} = \frac{k^s_1}{k^s_{-1}} \quad (9)$$

Thus, the reversible enantiomerization reactions which take place in the stationary phase during the time interval Δt are described by the simplified equation:

$$p_s(t_2) = \frac{K_p}{K_q + K_p} [p_s(t_1) + q_s(t_1)] +$$

$$+ \left\{ p_s(t_1) - \frac{K_q}{K_p + K_q} [p_s(t_1) + q_s(t_1)] \right\} \cdot \exp \left(- \frac{K_p + K_q}{K_q} \cdot k^s_1 \, \Delta t \right) \quad (10)$$

As a consequence of the detailed mass balance in the stationary phase during the enantiomerization step it follows that:

$$p_s(t_1) + q_s(t_1) = p_s(t) + q_s(t) = p_s(t_2) + q_s(t_2) \tag{11}$$

Since enantiomerization has been excluded from occurring in the mobile phase, the concentrations of the solutes, p_m and q_m, remain constant during the time interval Δt:

$$p_m(t_2) = p_m(t_1) \tag{12}$$

$$q_m(t_2) = q_m(t_1) \tag{13}$$

According to eqn. 9 the rate constants for enantiomerization, k_1^s and $k^s{}_{-1}$, are different when enantiomer resolution occurs on the chiral stationary phase, that is, when the distribution coefficients differ, $K_q \neq K_p$. This consequence is not unreasonable in view of the fact that enantiomers become distinguishable when residing in a chiral environment. The notion, however, that the activation barrier is lower for the least interacting enantiomer, *i.e.*, $k_1^s > k^s{}_{-1}$ for $K_q > K_p$ is not immediately apparent. The reversible first-order enantiomerization reaction offers an instructive demonstration of the wrong conclusions which can be drawn when the principle of microscopic reversibility is ignored. Thus, if $k_1^s/k^s{}_{-1}$ in eqn. 9 is set equal to unity (instead of 3825/3209 = 1.192) in the simulation experiment depicted in Fig. 2, 80% of the introduced racemic mixture is calculated to be present as only one configurational isomer after passage through the chromatographic column. No such "enantioselective transformation" by chromatography has been observed thus far (*cf.*, Fig. 1, bottom). In contrast, however, when A and B are solutes other than enantiomers the error introduced when violating the detailed material balance will be difficult to appreciate from the expected ratio of eluted peaks. Obviously, reaction schemes previously advocated in reaction GC such as[7,8,12]

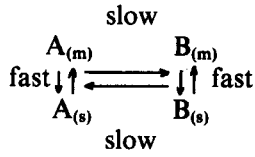

appear oversimplified and do not take into account the principle of microscopic reversibility.

To calculate a dynamic elution profile for interconverting enantiomers the three individual steps, that is, distribution, isomerization (enantiomerization) in the stationary phase and shift of the mobile phase —as represented by the above equations— are simulated via a computer program according to flow scheme I (*cf.*, Experimental). This procedure furnishes a digitally written chromatogram for p and q, respectively. Their combination yields the final interconversion profile which for given parameters, *i.e.*, the initial concentration ratio (usually 1:1), the retention times t for p and q, the dead-volume (gas hold-up time), t_M, the mean number of theoretical plates, $\bar{n}$, and the phase ratio, β, solely depends on the first-order rate constants of enantiomerization, k_1^s and $k^s{}_{-1}$, respectively.

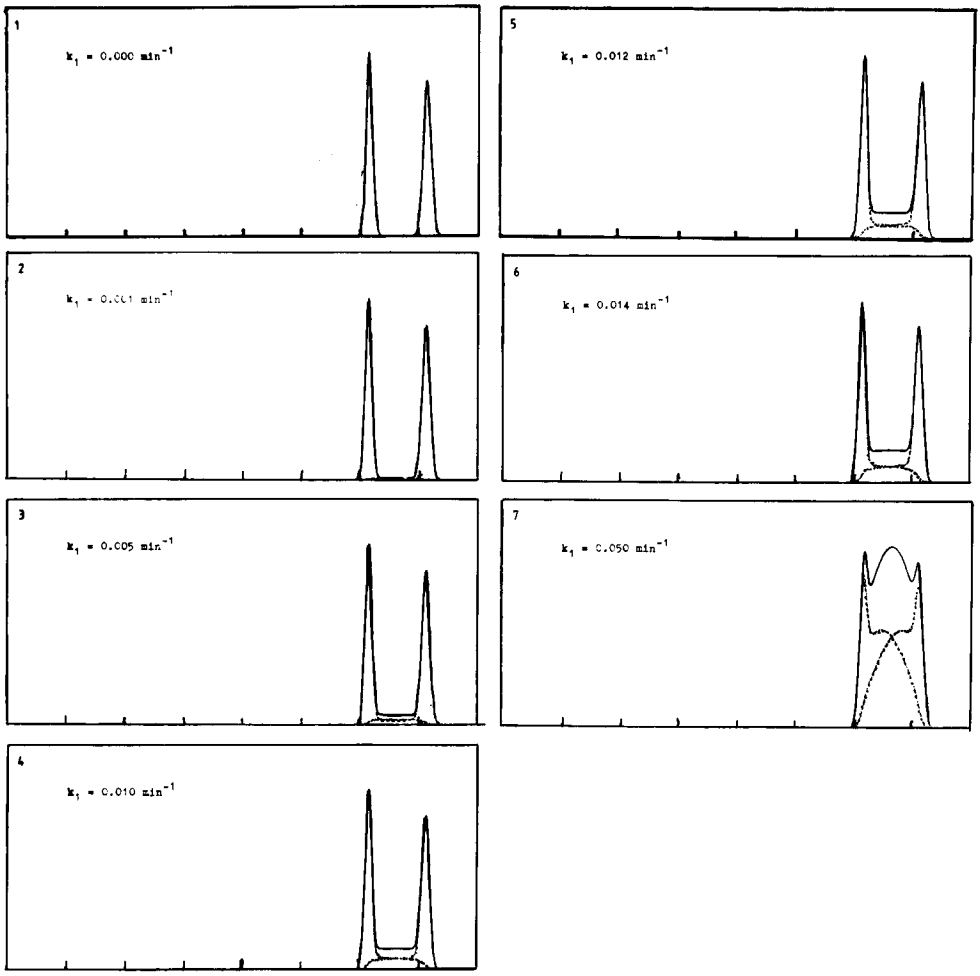

Fig. 2. Simulated gas chromatograms featuring enantiomerization. Parameters entered in the computer: number of mean theoretical plates, $\bar{n}$ = 10,000; distribution coefficients, K_p = 3209 and K_q = 3825; phase ratio, β = 624; time unit, t_M = 7.0 min; variable, k_1^s.

Using the measured chromatographic parameters for the resolution of 1 in the presence of 2 in squalane and varying k_1^s, chromatograms have been simulated (*cf.*, Fig. 2). The comparison of the computed (Fig. 3, bottom) and the experimental chromatograms (Fig. 3, top) reveals excellent agreement. Thus, the simulated chromatograms shown in Fig. 2 offer a diagnostic tool for the recognition of configurational interconversion of enantiomers during a chromatographic process.

For the determination of the experimental first-order rate constant k_1^s for inversion of 1 a best fit between experimental and computed chromagrams may be carried out through the systematic variation of k_1^s via regression analysis. However, at low enantiomerization rates a more straightforward graphical approach may be applied to obtain k_1^s. In the course of simulation experiments on the inversion of 1 in the presence of 2 in squalane it has been found that the rate constant k_1^s is linearly

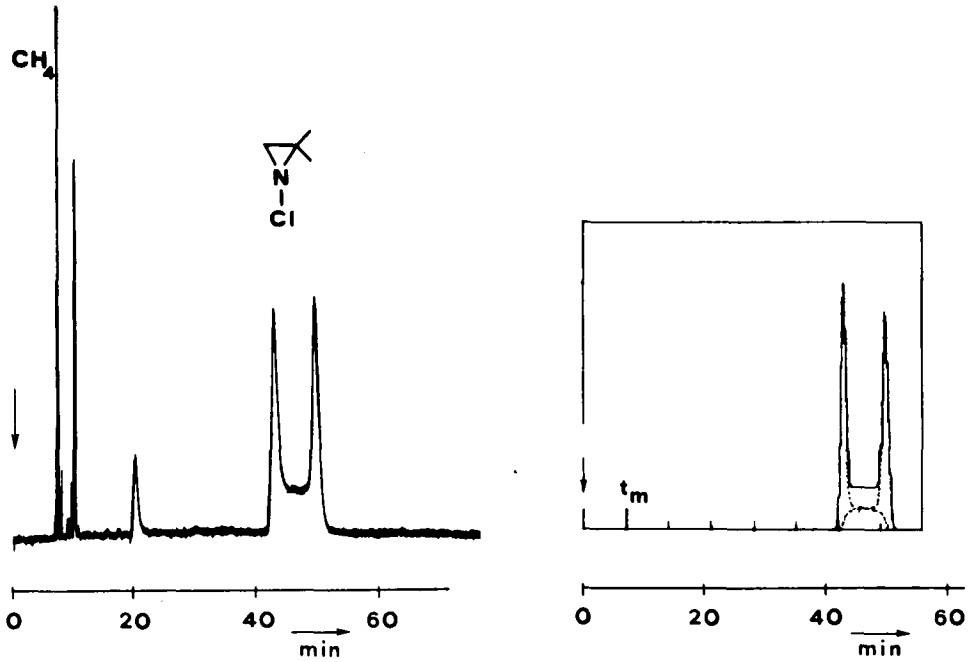

Fig. 3. Comparison of experimental and simulated gas chromatograms featuring enantiomerization. Left: peak coalescence (second kind) of 1 on 2 (0.133 M in squalane) at 60°C., 100 m × 0.5 mm nickel open-tubular column; carrier gas flow-rate, 2.8 ml/min; splitting ratio 1:50; peaks at 10 and 20 min are impurities. Right: simulated chromatogram with parameters taken from the experimental chromatogram; t_M = 7.0 min; K_p = 3209; K_q = 3825; β = 624; k_1 = 0.0141 min^{-1} = 2.35 · 10^{-4} sec^{-1}; ratio of peak heights, V_h = 0.187.

related to the ratio of the average height of the plateau, H_p, and the mean heights of the terminal peaks, H_t (*cf.*, Table I). The consideration of peak heights instead of peak areas (which are inaccessible due to peak overlap) appears to be justified since HETP has been chosen as the size of a section of the column in the present simulation

TABLE I

RATIOS OF PLATEAU HEIGHT AND MEAN HEIGHT OF TERMINAL PEAKS AND FIRST-ORDER RATE CONSTANTS FOR INVERSION FOR 1 AT 60°C TAKEN FROM THE SIMULATED CHROMATOGRAMS OF FIG. 2

Rate constant, k_1^1		*Height of the terminal peak (mm)*			*Medium plateau height,*	*Ratio of peak heights,*
min^{-1}	10^{-5} sec^{-1}	*Peak 1*	*Peak 2*	*Mean,* H_t	H_p *(mm)*	$V_h = H_p/H_t$
0.000	0.00	70.8	60.0	65.40	0.0	0.000
0.001	1.67	70.9	60.0	65.45	0.9	0.014
0.005	8.33	70.6	60.4	65.50	4.0	0.062
0.010	16.67	70.7	60.6	65.65	8.5	0.132
0.012	20.00	70.5	61.0	65.75	10.3	0.158
0.014	23.33	70.5	61.0	65.75	12.2	0.188

strategy. The graphical method is limited to elution profiles with horizontal plateau shapes. In fact, at higher rates of enantiomerization, the experimental and computed chromatograms resemble interconversion profiles in which the plateau grows to a broad and rounded hill whereas the terminal peaks gradually vanish (Fig. 2). By appropriate choice of the chromatographic conditions, *e.g.*, carrier gas flow, temperature, column length and metal chelate concentration, the occurrence of excessive peak coalescence can be prevented and hence the graphical method of determining k_1^s may then be employed.

We now proceed to calculate kinetic parameters for nitrogen inversion in 1-chloro-2,2-dimethylaziridine (1) in the presence of 2 [0.133 *M* (monomer) in squalane] at 60°C. With experimental data, *i.e.*, t_M = 7.0 min, t_p = 43.0 min, t_q = 49.9 min, β = 624 and $\bar{n}$ = 10,000, chromatograms are computer simulated (*cf.*, Fig. 2). The relationship between k_1^s and the ratio of the peak heights, $V_h = H_p/H_t$ (*cf.*, Table I), is linear with zero intercept (*cf.*, Fig. 4) which is represented by:

$$k_1^s = 7.56 \cdot 10^{-2}\,(\text{min}^{-1}) \cdot V_h = 1.26 \cdot 10^{-3}\,(\text{sec}^{-1}) \cdot V_h$$

From the experimental chromatogram, V_h = 0.187 is obtained graphically (*cf.*, Fig. 3). Assuming a graphical error in V_h of 10%, the rate constant of inversion in the stationary phase (s) is $k_1^s = (1.41 \pm 0.14) \cdot 10^{-2}\ \text{min}^{-1} = (2.35 \pm 0.24) \cdot 10^{-4}\ \text{sec}^{-1}$. From the general equation

$$\Delta G^{\neq} = -RT \cdot \ln(k_1 h/kT) = 4.57\,T\,(10.32 + \log T/k_1)\ \text{cal/mol}$$

and a transmission coefficient κ = 1 for nitrogen inversion, the free enthalpy of activation of enantiomerization of 1 in the presence of 2 in squalane at 60°C is $\Delta G^{\neq}$ = 104.9 ± 0.6 kJ/mol = 25.1 ± 0.1 kcal/mol. (The deviation of $\Delta G^{\neq}$ when calculated from k^s_{-1} (*cf.*, eqn. 8) lies well within the systematic error of $\Delta G^{\neq}$.)

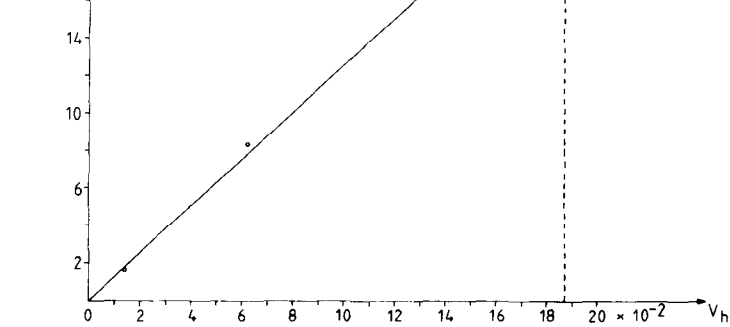

Fig. 4. Graphical correlation of k_1^s and V_h (data from Table I). With V_h = 0.187 (obtained from the upper chromatogram of Fig. 3) $k_1 = 2.35 \cdot 10^{-4}\ \text{sec}^{-1}$ is derived.

The present chromatographically obtained free enthalpy of activation for 1-chloro-2,2-dimethylaziridine (1) of $\Delta G^{\neq} = 25.1$ kcal/mol is reasonable in view of the fact that the activation barrier is diminished in the stationary phase, as verified experimentally (*vide supra*). The results are in agreement with that of Lehn and Wagner[16] who concluded from "dynamic" ^{1}H NMR investigations on 1 that $\Delta G^{\neq}$ must exceed 23.5 kcal/mol as no coalescence was detected below 180°C and with that of Kostyanovskii and Kadorkina[17] who determined a half-life, $\tau_{1/2} = 45$ min for partially enriched (+)−1 at 80°C, which corresponds to $\Delta G^{\neq} = 27.1$ kcal/mol.

CONCLUSIONS

The simulation treatment presented here has permitted the computation of peak shapes which occur when enantiomerization proceeds during resolution in a GC column. The simulated chromatograms represent a refined tool for diagnosis of configurational inversion in GC enantiomer separation as a source of error in the determination of enantiomeric compositions. It is demonstrated that the first-order rate constant and the free enthalpy of activation of enantiomerization may be obtained from readily accessible chromatographic parameters.

The merits of the GC method for the study of enantiomerization are:

the chiral solute need not be enantiomerically enriched; the racemic mixtures suffices

only trace quantities (10^{-8} g) of solute are required

impurities will in general be separated from the compound studied on the chromatographic column and, therefore, not interfere

highly volatile or gaseous solutes may be investigated

measurements can be performed over a wide and easily controllable temperature range

the method is rapid, simple, accurate and reproducible

The simulation treatment described may also be applied to the general case where the reversible first-order reaction occurs in both the gaseous and liquid phases. In view of the long computing time required, however, the application of the method should be confined to cases, as described herein, involving only one unknown independent rate constant, *i.e.*, that in the stationary phase. In principle, the treatment may be extended to any reversible first-order reaction such as constitutional rearrangement and configurational isomerism.

APPENDIX

Derivation of eqn. 6

Eqn. 6 is derived as follows. The kinetic law for configurational inversion of p is:

$$\frac{d[p_s(t)]}{dt} = -k_1^s\, p_s(t) + k_{-1}^s\, q_s(t)$$

The mass balance is constant in the stationary phase:

$$p_s(t) + q_s(t) = p_s(t_1) + q_s(t_1)$$

with $t_1 \leqslant t \leqslant t_2$

or

$$q_s(t) = p_s(t_1) + q_s(t_1) - p_s(t)$$

It follows that:

$$\frac{d[p_s(t)]}{dt} = -(k_1^s + k_{-1}^s)p_s(t) + k_{-1}^s[p_s(t_1) + q_s(t_1)]$$

This expression when integrated between t_1 and t_2 and $p_s(t_1)$ and $p_s(t_2)$ furnishes eqn. 6.

NOTE ADDED IN PROOF

The editor has drawn our attention to irreversible first order reactions, which involve radioactive elements eluting on paper (*e.g.*, ^{90}Sr–^{90}Y); calculations may be based on speed of development and half-lives of the elements. Elution profiles featuring enantiomerization have recently been observed in temperature-dependent chromatograms of racemates on triacetyl cellulose by liquid chromatography.

ACKNOWLEDGEMENTS

This work was supported by Fonds der Chemischen Industrie and by Deutsche Forschungsgemeinschaft. The authors thank Professors E. Gil-Av, The Weizmann Institute of Science, Israel, B. Karger, Northeastern University, Boston, U.S.A. and A. Mannschreck, Universität Regensburg, F.R.G., for their comments on the manuscript.

REFERENCES

1 E. Gil-Av, *J. Mol. Evol.*, 6 (1975) 131.
2 V. Schurig, *Chromatographia*, 13 (1980) 263.
3 I. S. Krull, *Advan. Chromatogr.*, 16 (1978) 175.
4 V. A. Davankov, *Advan. Chromatogr.*, 18 (1980) 139.
5 G. Blaschke, *Angew. Chem., Int. Ed. Engl.*, 19 (1980) 13.
6 V. Schurig, W. Bürkle, A. Zlatkis and C. F. Poole, *Naturwissenschaften*, 66 (1979) 423.
7 S. H. Langer, J. Y. Yurchak and J. E. Patton, *Ind. Eng. Chem.*, 61 (1969) 10.
8 S. H. Langer and J. E. Patton, *Advan. Anal. Chem. Instrumen.*, 11 (1973) 293.
9 V. Schurig and W. Bürkle, *J. Amer. Chem. Soc.*, 104 (1982) 7573.
10 F. Lefevre, T. Burgemeister and A. Mannschreck, *Tetrahedron Lett.*, (1977) 1125.
11 J. F. K. Huber, *Z. Anal. Chem.*, 277 (1975) 341.
12 R. A. Keller and J. C. Giddings, *J. Chromatogr.*, 3 (1960) 205.
13 A. J. P. Martin and R. L. M. Synge, *Biochem. J.*, 35 (1941) 1358.
14 D. W. Basset and H. W. Habgood, *J. Phys. Chem.*, 64 (1960) 769.
15 J. Kallen and E. Heilbronner, *Helv. Chim. Acta*, 43 (1960) 489.
16 J. M. Lehn and J. Wagner, *Chem. Commun.*, (1968) 148.
17 R. G. Kostyanovskii and G. K. Kadorkina, *Izv. Akad. Nauk SSSR, Ser. Khim.*, (1977) 1686.
18 V. Schurig, *J. Coord. Chem.*, 6 (1976) 63.